Atmospheric turbulence effects on the performance of a free space optical link employing orbital angular momentum multiplexing

Yongxiong Ren,[1,*] Hao Huang,[1] Guodong Xie,[1] Nisar Ahmed,[1] Yan Yan,[1] Baris I. Erkmen,[2] Nivedita Chandrasekaran,[3] Martin P. J. Lavery,[4] Nicholas K. Steinhoff,[5] Moshe Tur,[6] Samuel Dolinar,[2] Mark Neifeld,[7] Miles J. Padgett,[4] Robert W. Boyd,[8] Jeffrey H. Shapiro,[3] and Alan E. Willner[1]

[1]*Department of Electrical Engineering, University of Southern California, Los Angeles, California 90089, USA*

[2]*Jet Propulsion Laboratory, California Institute of Technology, Pasadena, California 91109, USA*

[3]*Massachusetts Institute of Technology, Research Laboratory of Electronics, Cambridge, Massachusetts 02139, USA*

[4]*School of Physics and Astronomy, University of Glasgow, Glasgow, G12 8QQ, UK*

[5]*The Optical Sciences Company, P.O. Box 25309, Anaheim, California 92825, USA*

[6]*School of Electrical Engineering, Tel-Aviv University, Tel-Aviv, 69978, Israel*

[7]*Department of Electrical and Computer Engineering, University of Arizona, Tucson, Arizona 85721, USA*

[8]*Department of Physics and Astronomy, The Institute of Optics, University of Rochester, Rochester, New York 14627, USA*

**Corresponding author: yongxior@usc.edu*

Received July 29, 2013; accepted August 28, 2013;
posted September 10, 2013 (Doc. ID 194300); published October 7, 2013

We experimentally investigate the performance of an orbital angular momentum (OAM) multiplexed free space optical (FSO) communication link through emulated atmospheric turbulence. The turbulence effects on the crosstalk and system power penalty of the FSO link are characterized. The experimental results show that the power of the transmitted OAM mode will tend to spread uniformly onto the neighboring mode in medium-to-strong turbulence, resulting in severe crosstalk at the receiver. The power penalty is found to exceed 10 dB in a weak-to-medium turbulence condition due to the turbulence-induced crosstalk and power fluctuation of the received signal.

OCIS codes: (010.1330) Atmospheric turbulence; (060.2605) Free-space optical communication; (060.4230) Multiplexing.
http://dx.doi.org/10.1364/OL.38.004062

The multiplexing of multiple orbital-angular-momentum (OAM) beams has emerged as a possible approach for increasing system capacity and spectral efficiency (SE) in free space optical (FSO) links [1–3]. Light beams carrying OAM can be described in the spatial phase form of $\exp(il\varphi)(l = 0, \pm1, \pm2, \ldots)$, in which φ refers to the azimuth angle and l determines the OAM value [4]. One key characteristic of beams carrying OAM is that they have a helical phase-front and "doughnut" intensity shape when $l \neq 0$, and they lie within an unbounded mode space (i.e., l can take any integer value) with each mode orthogonal to all of the others [1,5]. This suggests that efficient multiplexing and demultiplexing of multiple independent and spatially overlapping data-carrying OAM beams could be performed with negligible crosstalk [3,5].

Recent reports of FSO communication systems using OAM multiplexing have shown (1) a 2.56 Tbit/s data transmission link with an SE of 95.7 bit/s/Hz by multiplexing 32 OAM modes [3] and (2) a free space data link with a total capacity of 100.8 Tbit/s using OAM mode division multiplexing combined with wavelength division multiplexing [6]. However, these demonstrations are limited to fairly short distances, such that all the multiplexed beams are fully collected because their beam sizes do not exceed the receiver aperture's diameter in the absence of turbulence. It is known that inhomogeneities in the temperature and pressure of the atmosphere lead to variations of the refractive index along the transmission path. Given that there are multiple copropagating beams and that the orthogonality depends on the helical phase-front, these refractive index inhomogeneities will cause both degradation of a single OAM channel and intermodal crosstalk between different data channels with different OAM values [7–10], as shown in Fig. 1. Under dynamic turbulent atmosphere conditions, these degradations are slowly time-varying processes with time scale on the order of milliseconds (much slower than the signaling period) [11], which might severely limit the distance and number of OAM beams that can be accommodated in FSO links [12,13].

In this Letter, we experimentally investigate the effects of turbulence on the crosstalk and system power penalty in an OAM multiplexed FSO link. Rotating phase screen

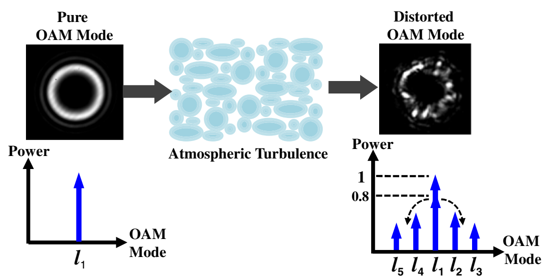

Fig. 1. Concept diagram of the effects of atmospheric turbulence on an OAM beam. A distorted OAM mode can be decomposed into multiple OAM modes [5].

plates with pseudorandom phase distributions obeying Kolmogorov spectrum statistics [11] are used to simulate moving turbulence in the laboratory environment. Our results show that turbulence will significantly spread the OAM power onto neighboring modes at medium-to-strong turbulence strengths, resulting in severe crosstalk at the receiver [13]. Consequently the system bit-error rate (BER) exhibits an error-floor phenomenon, and the power penalty is found to exceed 10 dB even under weak turbulence conditions.

The experimental setup is shown in Fig. 2. A 1550 nm laser is sent to a thermally stable Mach–Zehnder modulator with a nested Mach–Zehnder interferometer structure to produce a 40 Gbit/s quadrature phase-shift keying (QPSK) signal. The QPSK signal is amplified via a high-power erbium-doped fiber amplifier (EDFA) and filtered with a 2 nm bandwidth filter. The signal is then split into two paths, delayed relative to each other with fibers, and then delivered as two collimated Gaussian beams. These Gaussian beams (3 mm beam size) are then converted into three OAM beams with OAM values $l = 1$, 3, 5 by two reflective spatial light modulators (SLMs) loaded with specific spiral phase patterns. SLM-1 generates OAM $l = 3$, and by loading a superposition of two spiral phase patterns, SLM-2 generates OAM $l = 1$, 5 simultaneously. To separate the OAM beams from the residual unmodulated Gaussian beam, a blazed "fork" pattern, which is a combination of the imposed pattern and a linear phase ramp, was employed. The resulting OAM beams are then combined together to form a concentric ring and expanded by a telescope system (lens 1, 2) before passing through the turbulence emulator.

The effects of turbulence are emulated by a thin phase screen plate that is mounted on a rotation stage and placed in the middle of the optical path. The pseudorandom phase distribution which obeys Kolmogorov spectrum statistics and is characterized by the effective Fried coherence length, r_0, was machined into the plate [14,15]. The strength of the simulated turbulence can be varied by changing to a plate with a different r_0, changing the size of beam that is incident on the plate, or changing the number of passes through the plate. As the turbulent atmosphere also varies with time, it will lead to fluctuations of the received intensity and phase that are temporally correlated with cutoff frequency (correlation bandwidth) at about 0.1–1 kHz [11]. This frequency of the turbulence emulator can be adjusted by changing the incident position of the beam or the rotation speed [14].

To relate the parameters of the emulated link to a practical atmospheric link, it is required that the Rytov variance σ_R^2, D/r_0, and Fresnel number $D^2/\lambda L$ of the practical link equal the corresponding estimated values of the lab link [15]. Here λ denotes the wavelength, L is the link distance, and D is aperture diameter of the link, which can be obtained by measuring the beam diameter incident onto the phase plate. For a thin-screen model represented by the turbulence emulator of the setup [11], the effective atmospheric structure constant $\tilde{C}_n^2$ of the lab link is given by

$$\tilde{C}_n^2 = C_n^2 d = 2.36\left(\frac{\lambda}{2\pi}\right)^2 r_0^{-5/3},$$

where C_n^2 is the actual structure constant and d is the thickness of the phase screen. Then the Rytov variance for this link can be expressed as $\sigma_R^2 = 0.56(2\pi)^{7/6}\tilde{C}_n^2(L/4)^{5/6}$ [15,16]. This formula is valid for the case of a spherical wave and also holds in this experiment. With these parameters, a practical link can be adequately represented by the setup.

The beams exiting from the turbulence emulator are directed for measurements of average Strehl ratio, intensity distribution, crosstalk, and BER through three flip mirrors (FM1–3). Note that as the phase screen plate is rotated, passing through successive uncorrelated representations of turbulence, these measured signals will fluctuate temporally. Figure 3 presents the measured distribution of the received signal and the average Strehl ratio of the received images in order to verify the reliability and accuracy of the emulated turbulence. The phase plate, rotated at 40 rpm, leads to a cutoff frequency of about 10 Hz. It should be pointed out that in this case, the patterns loaded onto the SLMs were changed to a diffraction grating pattern to transmit the Gaussian beam (OAM $l = 0$). The beam reflected from FM-2 is detected,

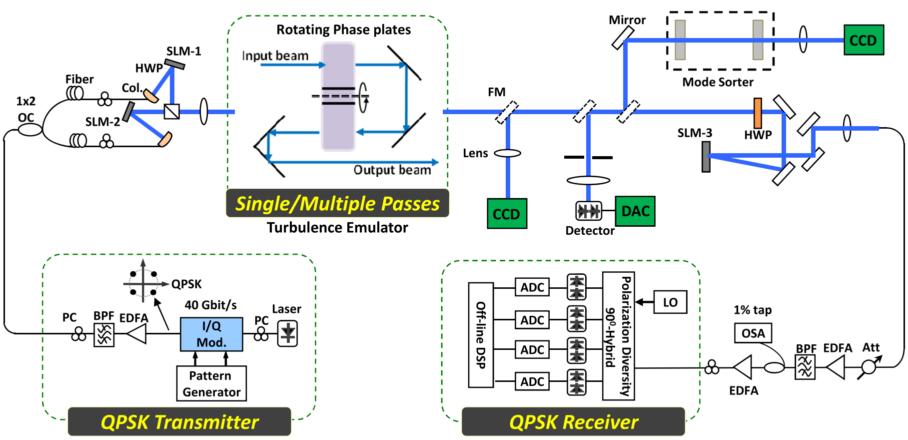

Fig. 2. Experimental setup of an OAM multiplexed FSO communication system. BPF, bandpass filter; Col., Collimator; EDFA, erbium-doped fiber amplifier; FM, flip mirror; DAC, digital–analog converter; DSP, digital signal processing; HWP, half-wave plate; LO, local oscillator; OC, optical coupler; PC, polarization controller; QPSK, quadrature phase shift keying.

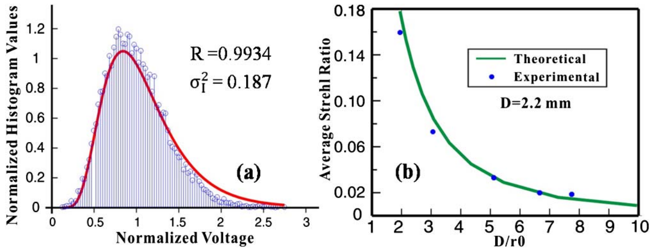

Fig. 3. (a) Normalized histograms of experimental data samples and lognormal fitting curves (red line) when transmitting Gaussian beam (OAM $l = 0$); The scintillation index σ_I^2 is 0.187 with a correlation coefficient $R = 0.9934$. (b) Average Strehl ratio of the received images. The measured beam diameter incident onto the phase screen plate is $D = 2.2$ mm.

digitized, recorded by an oscilloscope and subsequently processed to calculate the mean intensity and the scintillation index. As shown in Fig. 3(a), the probability density function of the intensity signal is verified to follow a lognormal model with a correlation coefficient $R = 0.993$, and the scintillation index σ_I^2 is found to be 0.187. The average Strehl ratio of the received images as a function of turbulence strength D/r_0 is depicted in Fig. 3(b). It is observed that the measured results are in reasonable agreement with the theoretical predictions which can be expressed as $[1 + (D/r_0)^{5/3}]^{-(6/5)}$.

To examine the atmospheric turbulence effects on an OAM beam, we characterized the modal crosstalk by measuring the power of the distorted beam in each OAM mode using an OAM mode sorter [17]. The mode sorter, which consists of two refractive elements, can transform both the phase and intensity of the beam in the form $\exp(il\varphi)$ to give a complex amplitude at the output plane of the form $\exp(ilx/a)$, where a is a scaling parameter [17]. A lens is used to focus these transformed states into specified lateral positions at a CCD placed in its focal plane, allowing for the efficient measurement of multiple OAM states simultaneously [16]. Adjacent equal-size regions are selected on the CCD image, with each region corresponding to a specific OAM mode. The sum of the measured pixel values in each of these regions is proportional to the power of the distorted beam in each OAM mode.

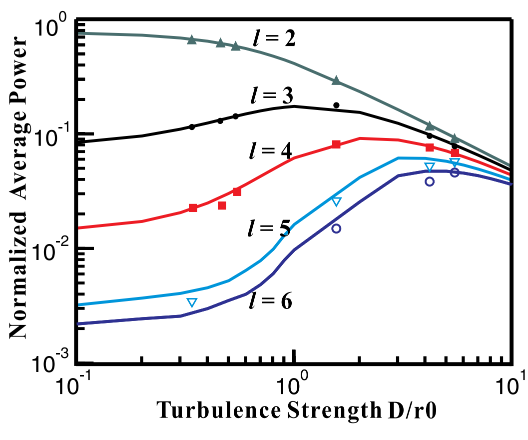

Fig. 4. Normalized average power in detected modes as a function of turbulence strength D/r_0 for an input mode $l = 2$. The solid lines are theoretical predications taking into account the inherent crosstalk of the mode sorter [16].

Figure 4 depicts the measurement (obtained from the mode sorter) of normalized average power (with respect to the power of transmitted mode) in each detected mode for a transmitted mode $l = 2$, with each data point representing the average of 250 measurements (the exposure time is 2 ms) with the phase plate rotating. In this case, only $l = 2$ is transmitted by programming SLM-1. The theoretical calculation predicted by [8] is also shown. One can see that the experimental points match the previous theoretical prediction [8,9]. It is also observed that as the turbulence strength increases, the power of transmitted OAM $l = 2$ is leaked to neighboring modes and tends to be equally distributed among modes for stronger turbulence. Note that the power in OAM $l + n$ equals the power in OAM $l - n$, which is not explicitly shown in the figure. To further illustrate this crosstalk behavior, the normalized average powers for $l = 0$ (upper) and $l = 3$ (lower) under different emulated turbulence conditions are plotted in Fig. 5. The parameters of an equivalent 1 km long real atmospheric link which would produce the same measurement statistics, including Rytov variance σ_R^2, Fresnel number F, and atmospheric structure constant $\tilde{C}_n^2$, are also given. We can see that the majority of the power is still in the transmitted OAM mode under weak turbulence but it spreads to neighboring modes as the turbulence strength increases. As the divergence of OAM mode is directly related to l, the size of the beam incident on the phase screen plate is larger for OAM $l = 3$, indicating that it will experience stronger turbulence distortions, as shown in Fig. 5.

Figure 6 shows the measured average BER under different turbulence strengths when (1) transmitting only OAM channel $l = 3$, and (2) transmitting three multiplexed OAM channels $l = 1, 3, 5$, to illustrate the crosstalk effects from adjacent channels (for simplification, channels $l = 1, 5$ transmit the same data). It can be seen that the turbulence-induced signal fading and crosstalk degrade the system performance dramatically. The power penalty at a forward-error-correction limit of 1×10^{-3} is ~1.3 dB for $D/r_0 = 0.42$, and >7 dB for both

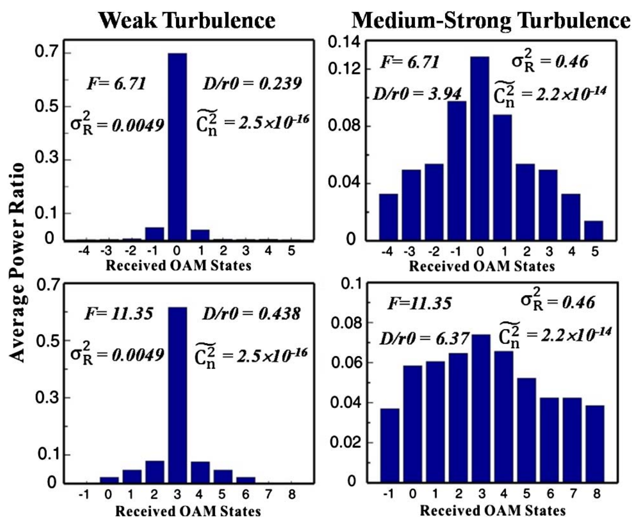

Fig. 5. Average power ratio on neighboring OAM channels when transmitting modes $l = 0$ (upper) and $l = 3$ (lower) under different emulated turbulence conditions.

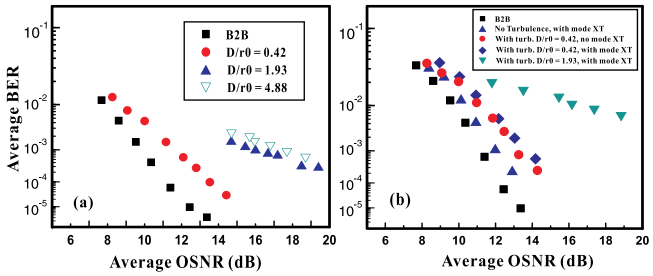

Fig. 6. Average BER under different turbulence strengths when transmitting (a) only OAM mode $l = 3$ and (b) three OAM multiplexed channels $l = 1$, 3, 5. OSNR: optical signal-to-noise ratio.

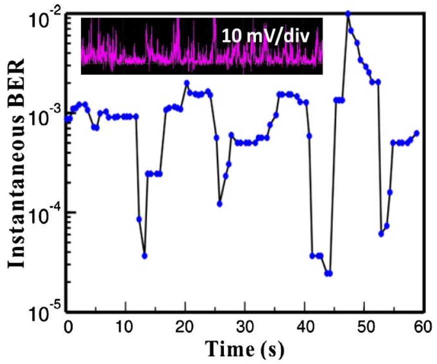

Fig. 7. Instantaneous BER of OAM channel $l = 3$ over 60 s at turbulence strength of $D/r_0 = 1.93$ with a fixed transmitted power. The inset illustrates the received signal fluctuation.

$D/r_0 = 1.93$ and 4.88 if OAM $l = 3$ is transmitted, as shown in Fig. 6(a). In this case, there is no crosstalk from other channels; hence the power penalty is mainly caused by turbulence-induced power fluctuations and the decreased average power received in the channel $l = 3$. When transmitting OAM channels $l = 1, 3, 5$ simultaneously, the average BER of channel $l = 3$ starts to exhibit an error-floor phenomenon as the turbulence strength increases, as shown in Fig. 6(b). With the strong crosstalk from the adjacent channels $l = 1, 5$, the average BER can barely approach 1×10^{-3} even at high optical signal-to-noise ratio (OSNR), and the system power penalty is found to be >10 dB for $D/r_0 = 1.93$.

As the phase screen is rotated, the beam passing through it experiences varying wavefront distortion that leads to time-dependent signal fading and crosstalk for the received signal [18]. To exhibit this behavior, Fig. 7 shows the instantaneous BER points of channel $l = 3$ over 60 s at $D/r_0 = 1.93$ in the absence of crosstalk from other channels. One can see that the instantaneous BER fluctuates temporally and the link will experience outage (BER $>1 \times 10^{-3}$) in strong turbulence fading.

In this Letter, we have experimentally studied the performance of an OAM-multiplexed FSO link through atmospheric turbulence. The turbulence effects on the crosstalk and system BER were investigated. The experimental results indicate that turbulence-induced signal fading and crosstalk will significantly deteriorate link performance and cause link outage in strong turbulence. Important future work would be to design an adaptive optics system to optically compensate these turbulence effects on the OAM beams.

We acknowledge the support of DARPA under the InPho (Information in a Photon) program.

References

1. G. Gibson, J. Courtial, M. Padgett, M. Vasnetsov, V. Pas'ko, S. Barnett, and S. Franke-Arnold, Opt. Express **12**, 5448 (2004).
2. T. Su, R. P. Scott, S. S. Djordjevic, N. K. Fontaine, D. J. Geisler, X. Cai, and S. J. B. Yoo, Opt. Express **20**, 9396 (2012).
3. J. Wang, J.-Y. Yang, I. M. Fazal, N. Ahmed, Y. Yan, H. Huang, Y. Ren, Y. Yue, S. Dolinar, M. Tur, and A. E. Willner, Nat. Photonics **6**, 488 (2012).
4. L. Allen, M. W. Beijersbergen, R. J. C. Spreeuw, and J. P. Woerdman, Phys. Rev. A **45**, 8185 (1992).
5. A. Yao and M. Padgett, Adv. Opt. Photon. **3**, 161 (2011).
6. H. Huang, G. Xie, Y. Yan, N. Ahmed, Y. Ren, Y. Yue, D. Rogawski, M. Tur, B. Erkmen, K. Birnbaum, S. Dolinar, M. Lavery, M. Padgett, and A. Willner, *Conference on Optical Fiber Communications* (OFC, 2013), paper OTh4G.5.
7. C. Paterson, Phy. Rev. Lett. **94**, 153901 (2005).
8. G. A. Tyler and R. W. Boyd, Opt. Lett. **34**, 142 (2009).
9. B. Rodenburg, M. P. J. Lavery, M. Malik, M. N. O'Sullivan, M. Mirhosseini, D. J. Robertson, M. Padgett, and R. W. Boyd, Opt. Lett. **37**, 3735 (2012).
10. J. A. Anguita, M. A. Neifeld, and B. V. Vasic, Appl. Opt. **47**, 2414 (2008).
11. L. Andrews and R. Phillips, *Laser Beam Propagation through Random Media*, 2nd ed. (SPIE, 2005).
12. N. Chandrasekaran, J. H. Shapiro, and L. Wang, Proc. SPIE **8518**, 851808 (2012).
13. Y. Ren, H. Huang, G. Xie, N. Ahmed, B. Erkmen, N. Chandrasekaran, M. Lavery, J. Shapiro, N. Steinhoff, M. Tur, M. Padgett, R. Boyd, and A. Willner, *Conference on Lasers and Electro-Optics* (CLEO, 2013), paper CM2G.4.
14. K. L. Baker, E. A. Stappaerts, D. Gavel, S. C. Wilks, J. Tucker, D. A. Silva, J. Olsen, S. S. Olivier, P. E. Young, M. W. Kartz, L. M. Flath, P. Krulevitch, J. Crawford, and O. Azucena, Appl. Opt. **43**, 5585 (2004).
15. P. Polynkin, A. Peleg, L. Klein, T. Rhoadarmer, and J. Moloney, Opt. Lett. **32**, 885 (2007).
16. L. Andrews, R. Phillips, and A. R. Weeks, Wave Random Media **7**, 229 (1997).
17. M. P. J. Lavery, D. J. Robertson, G. C. Berkhout, G. D. Love, M. J. Padgett, and J. Courtial, Opt. Express **20**, 2110 (2012).
18. V. W. S. Chan, IEEE Trans. Comm. **30**, 269 (1982).